

https://doi.org/10.1070/QEL16854

Fibre loop mirror with FBGs for the scanning range stabilisation in a fibre self-sweeping laser

A.Yu. Tkachenko, I.A. Lobach, E.V. Podivilov, S.I. Kablukov

Abstract. **A new scheme is suggested for stabilising scanning range boundaries of a self-sweeping fibre laser with fibre Bragg gratings (FBGs) and a fibre loop mirror. The mechanism for stabilising stop and/or start scanning boundaries is based on the formation of additional selective losses and/or reflection depending on the FBG position relative to the fibre mirror. It is shown that the simultaneous implementation of two selectors reduces fluctuations of the self-sweeping boundaries to several picometres, which is less by one-two orders in magnitude as compared with a case when the FBGs are absent. The approach suggested allows one to enhance predictability of emission wavelength tuning in fibre self-sweeping lasers, which is very important in practical applications.**

Keywords: *fibre laser, self-sweeping effect, fibre Bragg grating.*

1. Introduction

Wavelength-tunable lasers are widely employed in various fields of science and technique. In most cases, the laser frequency is tuned by adjustable spectral elements and drivers, which substantially complicate the laser design. In particular, Fabry–Perot interferometers [1], diffraction gratings or prisms [2], and tunable fibre Bragg gratings (FBGs) [3] are used for wavelength tuning. There are also papers in which the optical frequency is tuned by modulating laser parameters (for example, a pump current [4]). In addition, many works are devoted to developing a fibre laser with the frequency tuning based on Fourier domain mode locking, for example [5]. Previously [6, 7] it was shown that there is a class of fibre lasers with self-induced frequency sweeping (for simplicity, self-sweeping lasers), in which the emission frequency is tuned without employment of special spectral elements.

Operation of a self-sweeping laser is based on forming dynamic gratings of the refraction index and gain in the laser active medium [8, 9]. The spectral dynamics is directly related to that of laser intensity: the optical frequency changes stepwise from pulse to pulse by a value that is multiple of the cavity intermode beat frequency. In addition, there are schemes of a laser cavity [8], which realise a single-frequency self-sweeping regime where each pulse consists of a single longitudinal mode with a spectral width of ~ 1 MHz. Up to now, the self-sweeping has been demonstrated in various spectral ranges from 1.03 [6–8] to 2.1 μm [10]. A sufficiently simple scheme of such lasers allows them to compete with other tunable sources in many applications. Such lasers are used, in particular, for interrogation of fibre sensor lines based on FBGs [11] and analysis of laser spectra [12].

One of the key characteristics of tunable and self-sweeping lasers is the scanning range, which is determined as the absolute value of the difference of the start and stop wavelengths within a single scanning cycle. In practical applications of lasers, the tuning range and stability of range boundaries are also important. On an example of a self-sweeping Yb-laser [13] it was shown that the scanning range shifts to longer wavelengths if the active medium length increases or intracavity losses of the laser reduce. The scanning range can also be controlled by changing a temperature of the active medium. These approaches provide the scanning regime in the range of ytterbium gain profile from 1028 to 1080 nm. However, due to an uncontrollable character of the process, the range boundaries fluctuate from cycle to cycle, which complicates practical applications of such lasers. In order to solve the problem of scan boundary stabilisation it was suggested [14] for the laser output mirror to use the reflector based on a Michelson mode selector (MMS) formed by a fibre coupler, two FBGs, and fibre cleaved end. Depending on the FBG wavelength either the start or stop scanning boundary is stabilised. The MMS reflection spectrum is modulated in the range of FBG reflection. The stop boundary is stabilised due to the fact that in the scanning process, a successive mode fits the domain where MMS reflection is reduced, which is related with the interference of the waves reflected from the fibre end and from the FBG. In an instantenous jump to a short-wavelength range, the emission starts in a narrow reflection spectral band of the second FBG, which results in stabilisation of the start scanning boundary. However, since the reflection coefficient R of the output mirror is conventionally 0.1%–5% [6–14], the reflection coefficient of FBGs used for boundary stabilisation should be 0.01%–0.1%. At lower coefficients, the stabilisation was not observed, and at higher values the scanning only occurred in the FBG reflection spectral range. With standard FBGs (R = 10%–99%), small reflection coefficients were realised in [14] by using a fibre attenuator, which substantially reduced the laser output power.

In order to solve the scanning boundary stabilisation problem we suggest arranging the selective reflectors from the side of the highly reflective (HR) mirror. In this case, a high reflection coefficient of the HR mirror (as a rule it exceeds 50% for unidirectional laser emission) eliminates

A.Yu. Tkachenko Institute of Automation and Electrometry, Siberian Branch, Russian Academy of Sciences, prosp. Akad. Koptyuga 1, 630090 Novosibirsk, Russia; e-mail: alinka.tkacenko@yandex.ru; **I.A. Lobach, E.V. Podivilov, S.I. Kablukov** Institute of Automation and Electrometry, Siberian Branch, Russian Academy of Sciences, prosp. Akad. Koptyuga 1, 630090 Novosibirsk, Russia; Novosibirsk State University, ul. Pirogova 2, 630090 Novosibirsk, Russia

Received 9 October 2018; revision received 18 October 2018
Kvantovaya Elektronika **48** (12) 1132–1137 (2018)
Translated by N.A. Raspopov

stringent requirements on small reflection coefficients of the FBG. In this way, both the start and stop scanning wavelengths can be stabilised (depending on the selector position relative to the HR mirror). In particular, introduction of an FBG directly into a fibre loop mirror (FLM) results in a growth of selective losses [15], which promotes stabilisation of the stop scanning boundary. FBG placement in front of FLM causes a weak selective increase in the reflection coefficient and, thus, stabilises the start wavelength. With standard FBGs, such an approach makes it possible to reduce fluctuations of the scan boundaries from hundreds to several picometres. This is comparable with the results obtained with MMS [14].

2. Experiment

In the present work, a fibre self-sweeping Yb laser similar to [14] was used, in which a low reflecting FBG was replaced with a highly reflecting one that was moved to the side of the FLM (Fig. 1). Polarisation maintaining (PM) components were used in the laser. An active medium was an Yb-doped double-clad fibre (Nufern PM-YDF-5/130) of length 3 m coiled on the thermostable drum with controllable temperature. The pumping was realised through a pump combiner by the radiation of a laser diode (LD) with a wavelength of about 970 nm and power of 2 W. The laser cavity was formed by a HR broad-band FLM based on a polarising 50/50 coupler from one side and output reflector based on a right-angle-cleaved fibre from the other side. A substantial part of the radiation was extracted from the cavity through an 80/20 fibre coupler and isolator (providing true fibre output coupling). The laser generated a linearly polarised radiation due to the PM components and polarising FLM.

The laser operated in the single-frequency self-sweeping regime [8]. In addition, at high temperatures of the active fibre its scanning range shifted to the long-wavelength side [13]. Without FBGs inside the cavity, the heating of the active fibre from 20 to 45°C leads to the scanning boundaries shifting from $\lambda = 1056$ to 1066 nm and from $\lambda = 1077$ to 1083 nm for the start and stop values, respectively. In experiments on stabilising the scanning boundaries, the FBGs with the centre wavelengths of 1064 nm ($R \approx 27\%$, 55%, 85%) and 1080 nm ($R \approx 8\%$, 24%, 34%) were placed into the FLM and/or in front of it. The FBGs were formed in the PM fibre. The start and/or stop scanning boundary were stabilised depending on the FBG position relative to the HR mirror. In the experiment, long-time (more than 10 min) measurements of the temporal dynamics of a self-sweeping laser radiation wavelength were taken by using a fast HighFinesse/Angstrom laser spectrum analyser in various conditions.

2.1. Stabilisation of the stop scanning boundary

The stop scanning boundary was stabilised by adding into the FLM an FBG with a reflection centre wavelength close to the stop boundary of a selector-free laser. Similarly to [15], the FLM reflection spectrum exhibits additional dips related to the FBG. Moreover, the dips are additionally modulated due to wave interference in the FLM. The modulation period depends on the FBG position inside the FLM. For stabilising the stop boundary, we chose an FBG with a reflection centre wavelength of 1080.8 nm and reflection coefficient $R \sim 34\%$. At a temperature of the active fibre 25°C, the average value of the stop wavelength was ~1077 nm and FBG influence on the scanning process has not been observed (Figs 2a, 2d). In this case, absent stabilisation can be related to the fact that the FBG reflection range was not attained in the scanning. Indeed, the wavelength temporal dynamics was similar to that without an FBG, and the stop scanning boundary exhibited sufficiently large fluctuations (~200 pm). Circles in Fig. 3 denote the shift of the upper scanning boundary under heating of the active fibre. One can see that up to the active fibre temperature of 35°C the wavelength of the stop boundary increases. At temperatures above 35°C, the increase stops at a value corresponding to the FBG reflection wavelength, which testifies that the upper boundary is stabilised (Figs 2b and 2e). In this case, fluctuations of the stop boundary wavelength fall to ~9 pm. For comparison, Figs 2c and 2f present dynamics of a laser emission wavelength at a temperature of 45°C in the case of cavity without FBG. One can see that the stop boundary also has large fluctuations reaching ~110 pm, which confirms the necessity of FBG employment for stabilising it.

It was found that the stabilisation process depends on the FBG reflection coefficient. In particular, in contrast to the FBG with $R \sim 24\%$ and 34%, stabilisation of the stop boundary by the FBGs with $R \sim 8\%$ was not observed in the whole range of active fibre temperatures (20–45°C). In order to more exactly determine the FBG reflection coefficient needed for stabilisation, the radiation passed through the FLM was detected by a fast photodetector (see Fig. 1). As in [15], the transmission spectrum profile for the FLM with FBG coincided with that of the FBG reflection spectrum. Thus, once the temporal intensity dependence of the radiation passed through the FLM and the dynamics of laser wavelength are

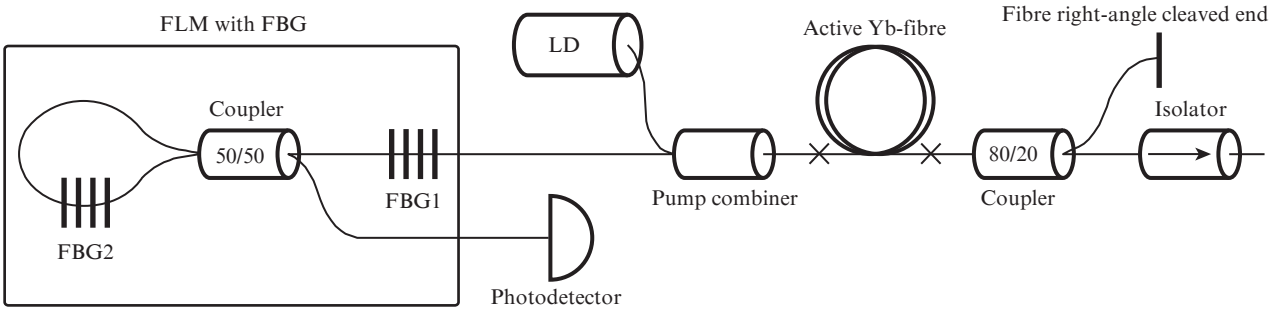

Figure 1. Schematic of a self-sweeping laser. FBG1, FBG2 are the gratings which stabilise the start and stop scanning boundaries, respectively.

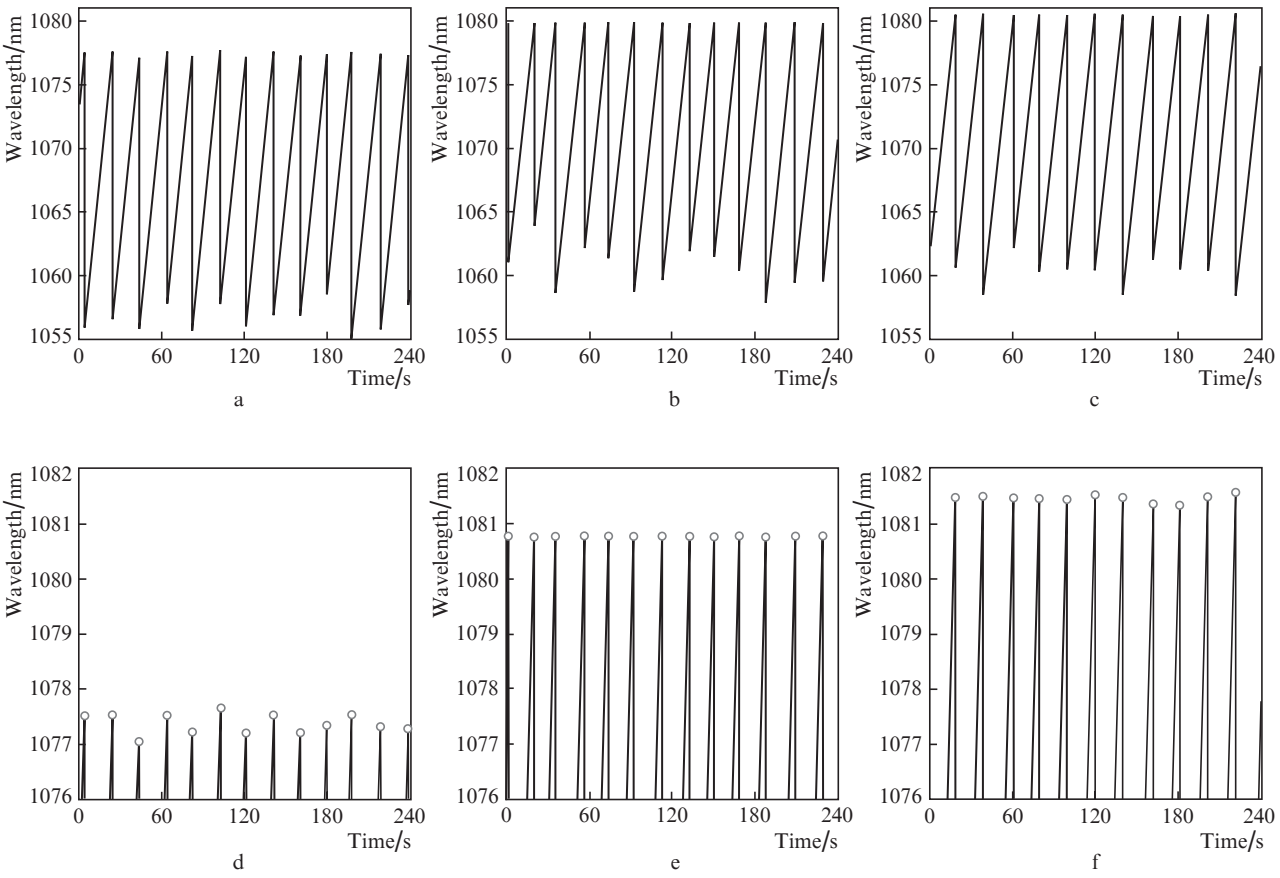

Figure 2. Temporal dynamics of the radiation wavelength of a laser with an FBG (λ = 1080.8 nm, $R \sim 34\%$) at (a) 25°C and (b) 45°C; without an FBG at 45°C (c). In Figs 2d, 2e, and 2f, parts of the same dependences are shown near the stop scanning boundary.

known, it is possible to recover the reflection spectrum of the used FBG [11]. Such measurements were taken for FBGs with $R \approx 8\%$, 24%, and 34% (Fig. 4). One can see that the temporal dependences of the radiation intensity for FBGs with $R \sim 34\%$ and 24% in Figs 4a and 4b, respectively, have sharp long-wavelength boundaries. This testifies that scanning breaks not having passed the whole FBG reflection spectrum and that the stop boundary is stabilised. However, an absent sharp boundary in the temporal intensity dependence of the radiation passed through the FLM in the case of FBG with $R \sim 8\%$ testifies that there is no stabilisation. FLM reflection spectra were measured by using a Yokogawa AQ6370 optical spectral analyser. Superimposed spectra of the radiation passed through the FLM with an FBG and FBG reflection spectra shows that the scanning breaks at $R \approx 15\%$ (Fig. 4). However, note that this value depends on experimental conditions (in particular, the temperature of active fibre was 45°C) and may change at a distinct temperature.

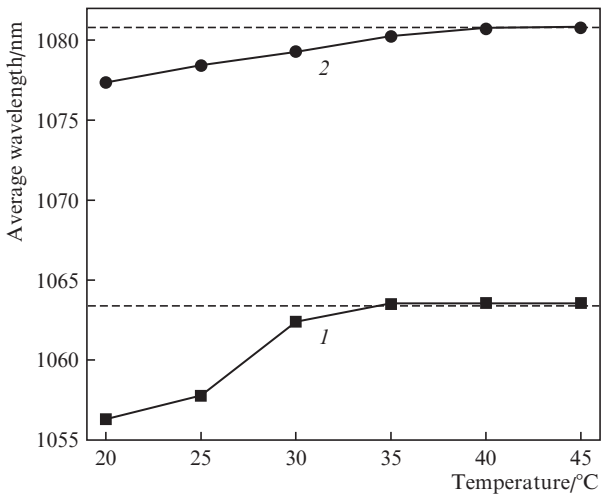

Figure 3. Temperature dependences of the start (*1*) and stop (*2*) boundaries of a scanning range with the employment of either FBG1 (λ = 1064 nm, $R \sim 27\%$), or FBG2 (λ = 1080.8 nm, $R \sim 34\%$), respectively. Dashed lines mark the centre wavelengths of FBG reflection.

This scheme was also used in measurements with the FBG having λ = 1064 nm. The character of the stop boundary stabilisation was different in this case. The stabilisation occurred only at low temperatures ~25°C (Fig. 5a). At a gradual temperature increase to 45°C, a jump of laser radiation wavelength over the FBG reflection spectrum was observed with a random value of a new start wavelength and the origin of a step in the wavelength-time dependence (Fig. 5b). It should be noted that such behaviour cardinally differs from that in the MMS scheme [14]. In that case, as the FBG reflection wavelength becomes shorter, the stop boundary stabilisation changes to stabilisation of the start boundary. However, the investigation of how the stability of the stop scanning boundary in the 'FLM with FBG' scheme depends on a centre wavelength of FBG reflection is beyond the scope of this work.

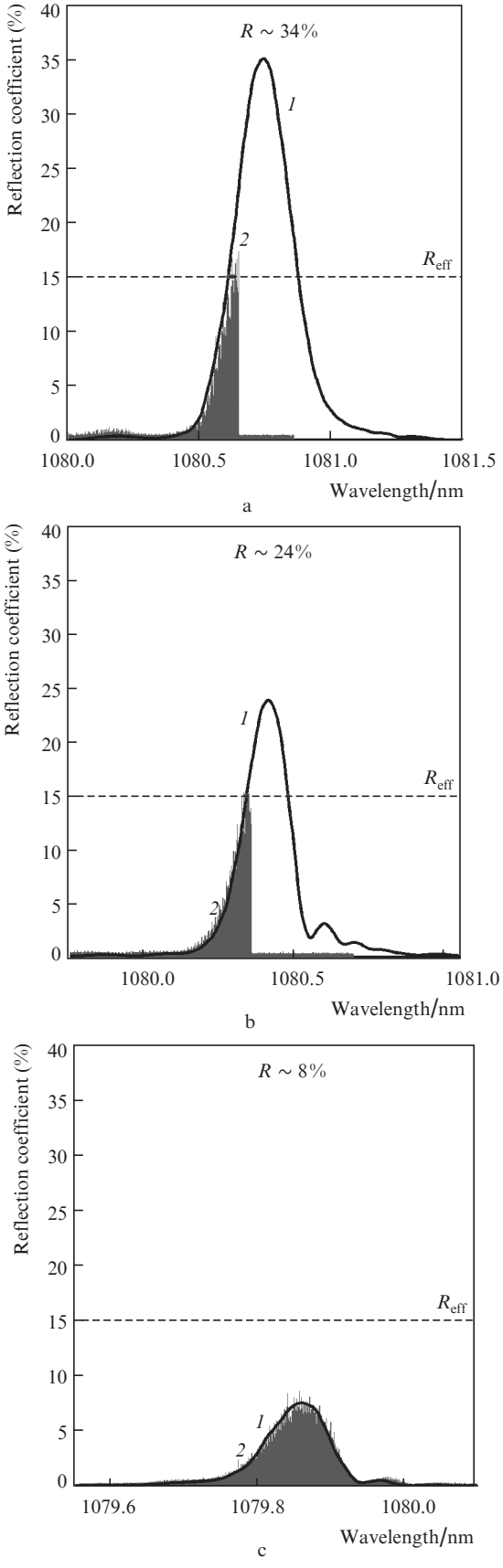

Figure 4. FBG reflection spectra (*1*) and time dependences of the intensity of radiation passed through FLM with an FBG (*2*) in the process of scanning at R = (a) 34%, (b) 24%, and (c) 8%. The temperature of active fibre is 45°C.

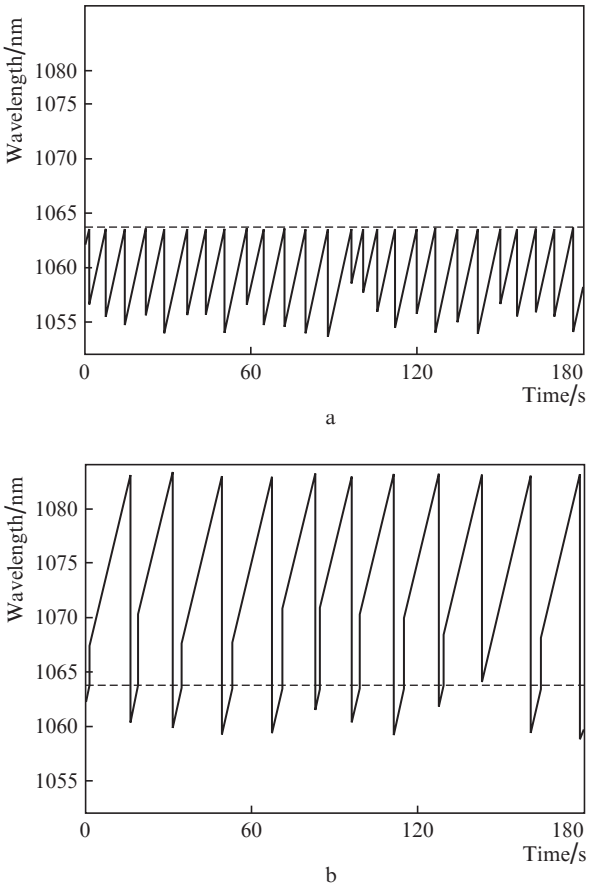

Figure 5. Temporal dynamics of the radiation wavelength of a laser with an FBG (λ = 1064 nm, $R \sim 85\%$) at temperatures of (a) 25°C and (b) 45°C.

2.2. Stabilisation of the start scanning boundary

In order to stabilise the start scanning boundary it is necessary to increase the reflection coefficient in a narrow spectral band. For this purpose, we place an FBG with the wavelength corresponding to the start scanning boundary in front of the FLM (see Fig. 1) and form a Fabry–Perot interferometer in the cavity. An FBG with λ = 1064 nm and $R \sim 27\%$ was chosen for this purpose. Similarly to the case of the stop boundary, the FBG did not affect the scanning process at the active fibre temperature of 25°C (Figs 6a and 6d). A temporal dynamics of the wavelength was similar to that in the case with an absent FBG, where the start scanning boundary exhibited large fluctuations ($\sim$1.8 nm). The scanning range was shifted by increasing the temperature of active fibre. In Fig. 3 one can see that a wavelength of the start boundary increases up to a temperature of 35°C. At higher temperatures when the start boundary reaches the wavelength of FBG reflection, the start boundary wavelength does not grow, which testifies that the boundary wavelength is related to the FBG reflection spectrum (Figs 6b and 6e). In this case, fluctuations of the start scanning boundary fall to $\sim$15 pm. For comparison, the dynamics of the laser radiation wavelength is shown in Figs 6c and 6f for a temperature of 45°C in the case of a cavity without an FBG. One can see that the start boundary also exhibits large fluctuations reaching $\sim$1.5 nm. Finally note, that, in contrast to the stop boundary, stabilisation of the start boundary was observed at all FBG reflection coefficients (from 27% to 85%) used in the experiments.

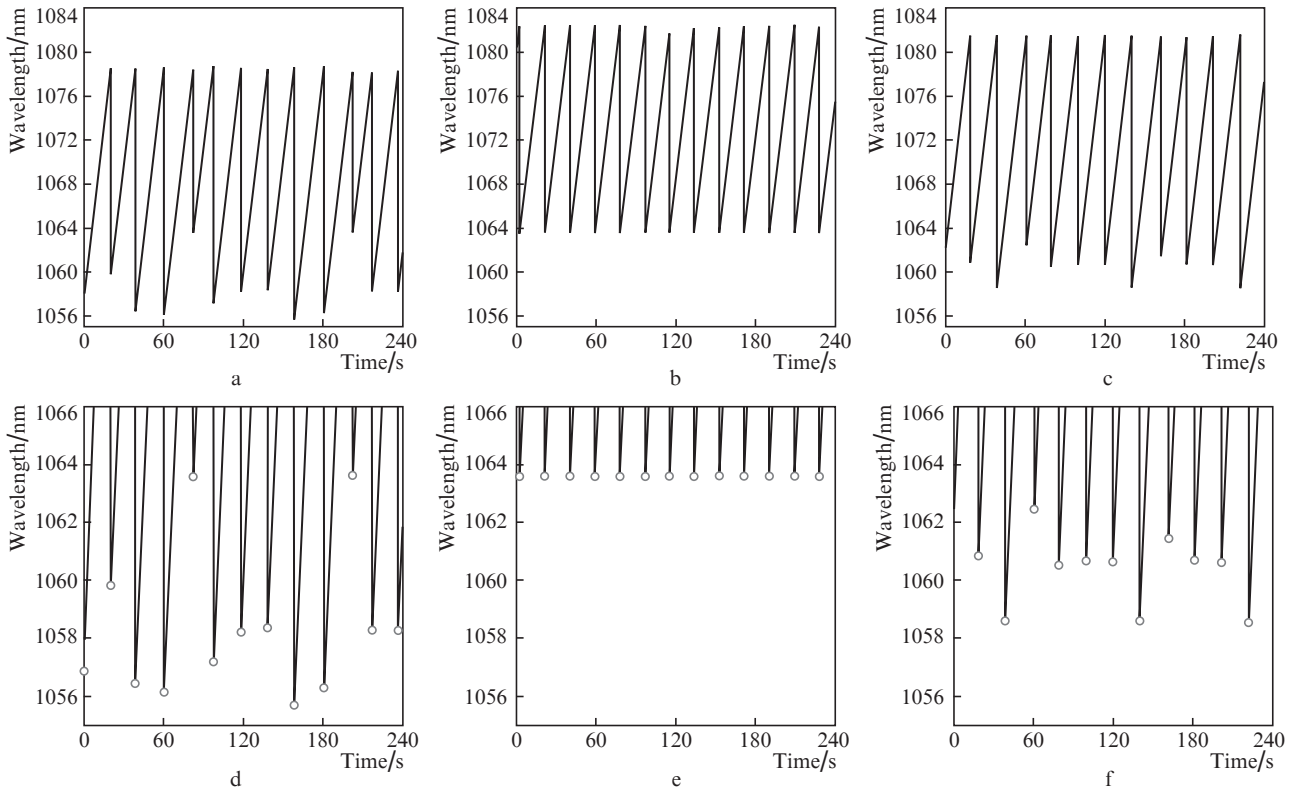

Figure 6. Temporal dynamics of the radiation wavelength of a laser with an FBG (λ = 1064 nm, $R \sim 27\%$) at temperatures of (a) 25°C and (b) 45°C, and without an FBG at 45°C (c). In Figs 6d, 6e, and 6f, parts of the same dependences are shown near the start scanning boundary.

2.3. Stabilisation of both scanning boundaries

From Fig. 3 one can see that the FBGs used make it possible to stabilise the scanning boundaries in the same temperature range from 35 to 45°C. This fact gives a chance to employ two FBGs for stabilising both boundaries simultaneously. For this purpose, two FBGs with λ = 1064 nm, $R \sim 27\%$ and λ = 1080.8 nm, $R \sim 34\%$ were arranged in the laser cavity (see Fig. 1). A temporal dynamics of the laser radiation wavelength is shown in Fig. 7 for the cases of a cavity without an FBG and cavity with two FBGs. One can see that without selective elements (Fig. 7a), the wavelengths of the start and stop scanning boundaries exhibit fluctuations of ~100 and 1500 pm, respectively. If two FBGs are placed into the cavity, fluctuations of the start and stop boundaries reduce to 9 and 6 pm, respectively (Fig. 7b).

In order to confirm the mechanism of scanning boundary stabilisation we have measured a transmission spectrum of the reflector used, which comprised an FLM and two FBGs (Fig 8). One can see that the additional FBG placed in front of the FLM reduces the transmission (that is, increases the reflection), whereas such an FBG arranged inside the FLM increases the transmission (reduces the reflection). It should be noted that the resolution of the employed Yokogawa AQ6370 optical spectrum analyser (0.02 nm) could not detect the modulation of transmission spectra due to formed enclosed interferometers, and the spectra presented are results of averaging. In addition, in the transmission coefficient measurements of the combined mirror we used the FBG with λ = 1064 nm and $R \sim 85\%$, whereas in the experiments with stabilisation of both the boundaries, the FBG reflection coefficient was less ($R \sim 27\%$). The reduction of the reflection coef-

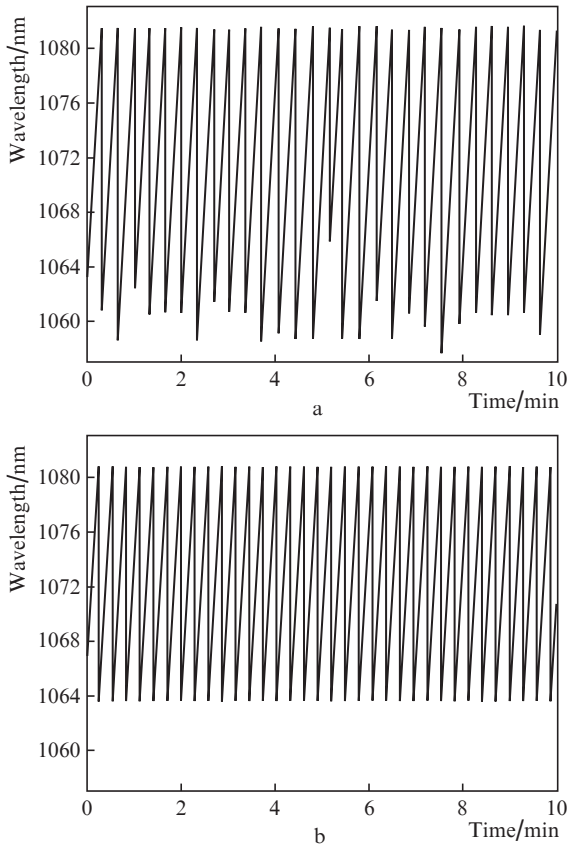

Figure 7. Temporal dynamics of the radiation wavelength of a self-sweeping laser (a) without an FBG and (b) with two FBGs.

ficient does not affect stabilisation of a scanning boundary, but the dip in the averaged transmission spectrum of the combined mirror at a wavelength of 1064 nm becomes comparable to a noise level. The dip in the spectrum testifies that the FBG placed in front of the FLM causes an additional selective reflection on the background of a broadband reflection from the HR mirror, which just favours formation of the start wavelength value of a scanning range. The FBG placed inside the FLM causes additional selective losses, which results in a wavelength jump (end of a sweeping cycle).

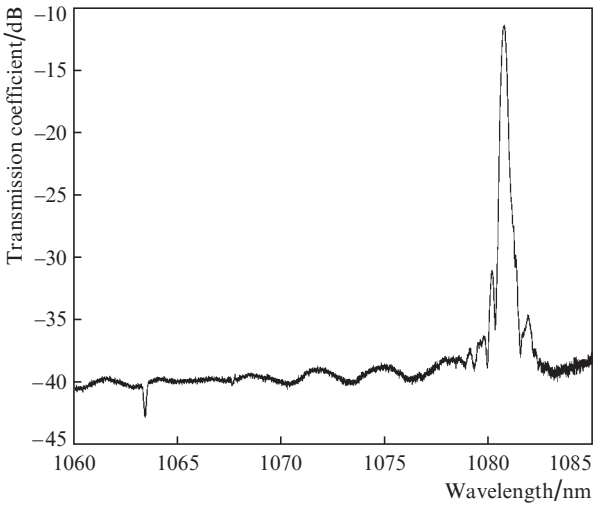

Figure 8. Transmission spectrum of FLM with two FBGs at $\lambda = 1064$ and 1080.8 nm.

3. Conclusions

A new scheme is suggested for stabilising the scanning boundaries in a self-sweeping fibre laser. The employment of spectral selectors in the form of an FBG from the side of the HR mirror allows one to stabilise as the start so and stop scanning boundaries. A selector arranged inside the highly reflecting fibre loop mirror results in additional selective losses, which favours stabilisation of the stop scanning boundary. The selector placed directly in front of the highly reflecting mirror favours stabilisation of the start scanning boundary. It is shown that the simultaneous employment of two selectors reduces fluctuations of both the scanning boundaries to picometre level, which is by one-two orders in magnitude less than without selectors. The approach suggested has an unassailable advantage over the stabilisation scheme with a selective output mirror realised in the Michelson configuration, where the requirements to a small reflection coefficient of used FBGs are very stringent.

The approach makes it possible to enhance the predictability of generation wavelength tuning (that is, wavelength determination from measurements of the time passed since a new scanning cycle) in fibre self-sweeping lasers, which is rather important in practical applications.

Acknowledgements. The authors are grateful to I.N. Nemov for fabrication of FBGs used in experiments. Experimental studies of A.Yu. Tkachenko are funded by the Russian Foundation for Basic Research (Grant No. 18-32-00563). The work is supported by the Ministry of Education and Science of the Russian Federation (Minobrnauka) (No. 0319-2018-0004) with the employment of facility from Multiple-Access Centre "High-resolution Spectroscopy of Gases and Condensed Matter" at the IA&E SB RAS, Novosibirsk, Russian Federation.

References

1. Dawson J.W., Park N., Vahala K.J. *Appl. Phys. Lett.*, **60**, 3090 (1992).
2. Kwon Y.S., Ko M.O., Jung M.S., Park I.G., Kim N., Han S.-P., Ryu H.-C., Park K.H., Jeon M.Y. *Sensors*, **13**, 9669 (2013).
3. Babin S.A., Kablukov S.I., Vlasov A.A. *Laser Phys.*, **17**, 1323 (2007).
4. Yamashita S., Takubo Y. *Photon. Sensors*, **3**, 320 (2013).
5. Jung E.J., Kim C.-S., Jeong M.Y., Kim M.K., Jeon M.Y., Jung W., Chen Z. *Opt. Express*, **16**, 16552 (2008).
6. Kir'yanov A.V., Il'ichev N.N. *Laser Phys. Lett.*, **8**, 305 (2011).
7. Lobach I.A., Kablukov S.I., Podivilov E.V., Babin S.A. *Opt. Express*, **19**, 17632 (2011).
8. Lobach I.A., Kablukov S.I., Podivilov E.V., Babin S.A. *Laser Phys. Lett.*, **11**, 045103 (2014).
9. Peterka P., Honzátko P., Koška P., Todorov F., Aubrecht J., Podrazký O., Kašík I. *Opt. Express*, **24**, 16222 (2016).
10. Navratil P., Peterka P., Vojtisek P., Kasik I., Aubrecht J., Honzatko P., Kubecek V. *Opto-Electron. Review*, **26**, 29 (2018).
11. Tkachenko A.Yu., Lobach I.A. *Prikladnaya Fotonika*, **3**, 37 (2016).
12. Tkachenko A.Yu., Lobach I.A., Kablukov S.I. *Opt. Express*, **25**, 17600 (2017).
13. Lobach I.A., Tkachenko A.Yu., Kablukov S.I. *Laser Phys. Lett.*, **13**, 045104 (2016).
14. Tkachenko A.Yu., Vladimirskaya A.D., Lobach I.A., Kablukov S.I. *Opt. Lett.*, **43**, 1558 (2018).
15. Shu X., Yu L., Zhao D., Zhang L., Sugden K., Bennion I. *J. Opt. Soc. Am. B*, **19**, 2770 (2002).